$$T = \begin{pmatrix} (\bar{B}_m - 1) + \bar{D}_1{*}\frac{\partial^2}{\partial r^2} & \bar{A}^2 \\ -\bar{B}_\mathrm{m} & -\bar{A}^2 + D_2\frac{\partial^2}{\partial r^2} \end{pmatrix} \qquad \text{(B.13)}$$

The solution of eq B.11 is given by

$$\begin{pmatrix} u_0 \\ v_0 \end{pmatrix} = \beta_1 \sin m\pi r\begin{pmatrix} 1 \\ \bar{\rho}_m \end{pmatrix} + \beta_2 \sin (m + 1)\pi r\begin{pmatrix} 1 \\ \bar{\rho}_{m+1} \end{pmatrix} \qquad \text{(B.14)}$$

The normalization condition is

$$(1 + \bar{\rho}_m{}^2)\beta_1{}^2 + (1 + \bar{\rho}_{m+1}{}^2)\beta_2{}^2 = 2 \qquad \text{(B.15)}$$

A necessary condition for the existence of a solution to eq B.12 is that the nonhomogeneous term be orthogonal to each of the solutions

$$\begin{pmatrix} u_0{}^* \\ v_0{}^* \end{pmatrix}$$

of the adjoint problem to eq B.10. This leads to

$$\beta_1 b_0 F(\bar{D}_1{}^*,D_2,m,f) = 0 \qquad \text{(B.16)}$$

$$\beta_2 H(\bar{D}_1{}^*,D_2,m,f,b_0) = 0 \qquad \text{(B.17)}$$

where

$$F = 1 - \bar{D}_1{}^*[2 + \pi^2\bar{D}_1{}^*m^2(m + 1)] + \frac{2}{3}[(m + 1)^2\pi^2\bar{D}_1{}^* + 1]m^3\pi^2(\bar{D}_1{}^*D_2)^{1/2}f \qquad \text{(B.18)}$$

$$H = -\frac{\pi^2\bar{D}_1{}^{*2}(2m + 1)}{m^2(m + 1)^2(2\bar{D}_1{}^* - f\bar{A})} + \frac{(2m + 1)\pi^4D_1{}^{*3/2}D_2{}^{1/2}}{2m(m + 1)(2\bar{D}^* - f\bar{A})}f + 4c_{1m}b_0\left(\frac{-1 + m^2(m + 1)^2\pi^4\bar{D}_1{}^{*2} + \pi^2\bar{D}_1{}^*(2m + 1)}{3m^2\pi^3(m + 1)(\bar{D}_1{}^*D_2)^{1/2}} + \frac{2(m + 1)[1 - m^2(m + 1)^2\pi^4\bar{D}_1{}^{*2}]}{m^2\pi^3(3m + 2)(m + 2)(\bar{D}_1{}^*D_2)^{1/2}} + \frac{1}{6}[(m + 1)^2\bar{D}_1{}^*\pi^2 + 1)m\pi f\right) \qquad \text{(B.19)}$$

Generally in an ideal system, one has

$$F \neq 0 \qquad \text{(B.20)}$$

Therefore, we can calculate the value of (β_1,β_2,b_0) from eq B.15–B.17, and each real triplet (β_1,β_2,b_0) yields a secondary bifurcating state. But in a nonideal system, the condition B.20 is not guaranteed a priori. In fact, when the nonideality parameter f takes some special values, one has $F = 0$. In this case, eq B.15–B.17 cannot determine uniquely the value of (β_1,β_2,b_0). This implies that $\delta^{1/2}$ in eq B.10 is not the appropriate expansion parameter. As a result, the behavior of secondary bifurcating branches will have a different dependence on parameters than in the ideal case.

Absolute Rate Constants for the Reactions of HCO with O_2 and NO from 298 to 503 K

B. Veyret* and R. Lesclaux

Laboratoire de Chimie Physique A, Université de Bordeaux I, 33405 Talence Cédex, France *(Received: December 1, 1980; In Final Form: February 27, 1981)*

The absolute rate constants for the reactions $HCO + O_2 \rightarrow HO_2 + CO$ and $HCO + NO \rightarrow HNO + CO$ have been determined by using a flash photolysis–laser resonance absorption technique. The values obtained at 298 K are in units of cm^3 $molecule^{-1}$ s^{-1}: $k_{O_2} = (5.6 \pm 0.6) \times 10^{-12}$ and $k_{NO} = (12.3 \pm 1.2) \times 10^{-12}$. Negative temperature coefficients have been found between 298 and 503 K for both reactions: $k_{O_2} = 5.5 \times 10^{-11} \times T^{-0.4\pm0.3}$ and $k_{NO} = 1.2 \times 10^{-10} \times T^{-0.4\pm0.3}$. Both formaldehyde and acetaldehyde were used as sources of formyl radicals. The total pressure was varied with no noticeable effect on the rate constants. Critical evaluation and recommendation are made in view of the previous results for use in atmospheric modeling.

Introduction

Several recent studies[1-4] have provided information about the reaction kinetics of the formyl radical HCO with the scavengers O_2 and NO. These reactions are of importance in the combustion of hydrocarbons and the photochemistry of the atmosphere.

Direct measurements of these rate constants using various techniques have remained so far in poor agreement and never included studies of the temperature dependence.

The first technique used was an indirect photoionization mass-spectrometry method by Washida et al.[1] They obtained a value for the rate constant of the reaction $HCO + O_2$ of $(5.7 \pm 1.2) \times 10^{-12}$ cm^3 $molecule^{-1}$ s^{-1}. This value was included in atmospheric simulations for some time and was later confirmed by Shibuya et al.,[2] who used flash photolysis and absorption spectroscopy techniques. Flash photolysis associated with intracavity dye laser spectroscopy (IDLS) were used by Reilly et al.[3] and Nadtochenko et al.[4] to study the same reaction. Both groups reported a lower k_{O_2} value of $\sim 4 \times 10^{-12}$ cm^3 $molecule^{-1}$ s^{-1}.

The reaction HCO + NO was studied by the IDLS technique, which yielded the value $k_{NO} \approx 13 \times 10^{-12}$ cm^3 $molecule^{-1}$ s^{-1},[3,4] while Shibuya et al.[2] had reported a lower value of $\sim 8.5 \times 10^{-12}$ cm^3 $molecule^{-1}$ s^{-1}.

In this paper we report measurements of both rate constants using flash photolysis in conjunction with ex-

---

[1] N. Washida, R. I. Martinez, and K. D. Bayes, *Z. Naturforsch. A*, **29**, 251 (1974).

[2] K. Shibuya, T. Ebata, K. Obi, and I. Tanaka, *J. Phys. Chem.*, **81**, 2292 (1977).

[3] J. P. Reilly, J. H. Clark, C. B. Moore, and G. C. Pimentel, *J. Chem. Phys.*, **69**, 4381 (1978).

[4] V. A. Nadtochenko, O. M. Sarkisov, and V. I. Vedeneev, *Dokl. Akad. Nauk SSSR*, **244**, 152 (1979).

0022-3654/81/2085-1918$01.25/0

tracavity dye laser absorption spectroscopy (EAS). These rate-constant measurements were made as a function of the scavenger concentration, the total pressure, the temperature, and the nature of the source of HCO (formaldehyde and acetaldehyde). The temperature measurements gave the first estimate of the activation energy for the reactions.

The photolysis of formaldehyde in the presence of a scavenger X proceeds according to the following reaction scheme:

$$H_2CO \xrightarrow{h\nu} H + HCO \text{ (or } H_2 + CO)$$

$$H + H_2CO \xrightarrow{k_1} H_2 + HCO \qquad (1)$$

$$H + HCO \xrightarrow{k_2} H_2 + CO \qquad (2)$$

$$HCO + HCO \xrightarrow{k_3} H_2CO + CO \qquad (3)$$

$$HCO + X \xrightarrow{k_x} HX + CO \qquad (4)$$

In the case of acetaldehyde, the reactions are

$$CH_3CHO \xrightarrow{h\nu} CH_3 + HCO \text{ (or } CH_4 + CO)$$

$$CH_3 + CH_3CHO \xrightarrow{k_5} CH_4 + CH_3CO \qquad (5)$$

$$CH_3 + HCO \xrightarrow{k_6} CH_4 + CO \qquad (6)$$

$$CH_3 + CH_3 \xrightarrow{k_7} C_2H_6 \qquad (7)$$

along with reactions 3 and 4.

Methyl radicals react essentially through the fast reactions 6 and 7, as reaction 5 is slow. In all experiments the radical concentrations were kept as low as possible in order to minimize the recombination processes, and pseudo-first-order conditions were used in the measurements of k_x. Contribution of the second-order processes was taken into account by means of a simple kinetic simulation. An initial HCO concentration of ca. 8×10^{13} cm^{-3} was estimated from experiments with no scavenger added and based on the k_3 value measured by Hochanadel et al.[5]

Experimental Section

The photolysis apparatus has been described previously.[6,7] Formyl radicals were generated in the flash photolysis of either formaldehyde or acetaldehyde. The photolysis cell was a cylindrical quartz tube fitted with antireflective coated windows, and it was placed in an oven. The temperature could be varied from 25 to 250 °C. Two cylindrical flash lamps were mounted parallel to the cell and delivered 110-J pulses of ~5-μs duration. The analyzing light was provided by a 580 Spectra Physics dye laser which was operated with rhodamine 6G and modified to accomodate a jet. The laser was tuned to the head of the absorption band of HCO at 614.5 nm. The bandwidth of the laser was small enough (~0.25 Å) compared to the width of the absorption line and the laser wavelength sufficiently stable to ensure proper absorption conditions. With the help of a multiple pass system, the optical path length for the dye laser beam through cell could be as long as 40 m, and absorption as low as 3% could be recorded in a single-shot experiment.

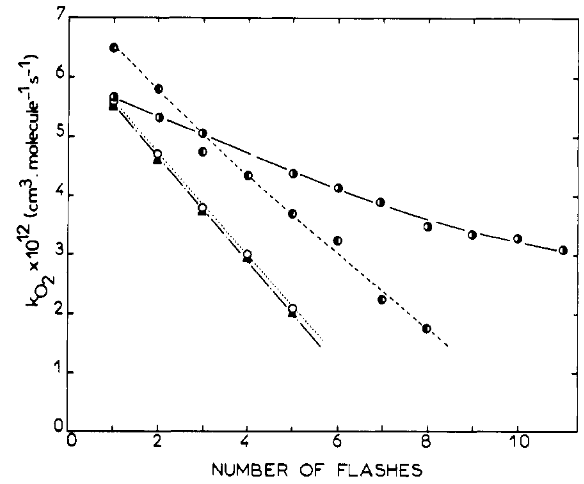

Figure 1. HCO absorbance decay (solid line) as a function of time after flash (H_2CO, 40 torr; 144 mtorr of O_2). Simulations done with $2k_3/(\epsilon d)$ = 52000 s^{-1} and $k_{O_2} = 5.0 \times 10^{-12}$, 5.6×10^{-12}, and 6.2×10^{-12} cm^3 molecule^{-1} s^{-1} for curves A, B, and C, respectively (dotted lines).

Formaldehyde was prepared according to the method of Spence and Wild,[8] distilled under vacuum at low temperature, and stored in liquid nitrogen. It was further purified by freeze-pump-thaw cycles before each experiment. Acetaldehyde (Fluka AG, 99.5%) was purified by trap-to-trap distillation, stored in the dark at 4 °C, and degassed before use. Oxygen (Air Liquide, 99.995%) was used with no further purification and diluted in nitrogen (Air Liquide, 99.999%). Nitric oxide (Air Liquide, 99.9%, with only N_2 as impurity) was stored over silica gel and diluted in N_2. A greaseless vacuum line was used to handle all gases. The empty photolysis cell was heated at 240 °C under vacuum for 2 h before each filling in order to prevent formaldehyde polymerization. Nevertheless, as formaldehyde pressure was above 10 torr, polymerization did occur, but slowly enough to allow for measurements to be made with no noticeable fogging of the windows or drop of the total pressure. However, at high total pressure, only acetaldehyde could be used as formaldehyde polymerization rapidly occurred in that case.

The pseudo-first-order conditions were achieved through the choice of experimental conditions. At large aldehyde concentration (~40 torr), the H-atom reactions 1 and 2 are much faster than reactions 3 and 4 involving HCO and X. Thus, shortly after the flash (~50 μs) all H atoms have disappeared and HCO radicals are left to react with X and with themselves. The energy of the photolyzing flash was such that the initial amount of HCO was as small as possible in order to minimize the second-order contribution of reaction 3. The scavenger concentrations were as large as possible to approximate pseudo-first-order conditions. However, as the second-order contribution could not be completely neglected, the HCO decay had to be simulated by solving the differential equation

$$-d[HCO]/dt = 2k_3[HCO]^2 + k_x[HCO][X] \qquad (8)$$

As the initial amount of HCO was not accurately known, the HCO absorbance A was used rather than [HCO]

$$-dA/dt = [2k_3/(\epsilon d)]A^2 + k_x[X]A \qquad (9)$$

where ϵ is the molar extinction coefficient of HCO and d

---

(5) C. J. Hochanadel, T. J. Sworski, and P. J. Ogren, *J. Phys. Chem.*, **84**, 231 (1980).

(6) P. V. Khe and R. Lesclaux, *J. Phys. Chem.*, **83**, 1119 (1979).

(7) R. Lesclaux, J. C. Soulignac, and P. V. Khe, *Chem. Phys. Lett.*, **43**, 520 (1976).

(8) R. Spence and W. Wild, *J. Chem. Soc.*, 335 (1935).

(9) J. H. Clark, C. B. Moore, and N. S. Nogar, *J. Chem. Phys.*, **63**, 1264 (1978).

(10) N. Washida, H. Akimoto, and M. Okuda, *J. Phys. Chem.*, **82**, 2293 (1978).

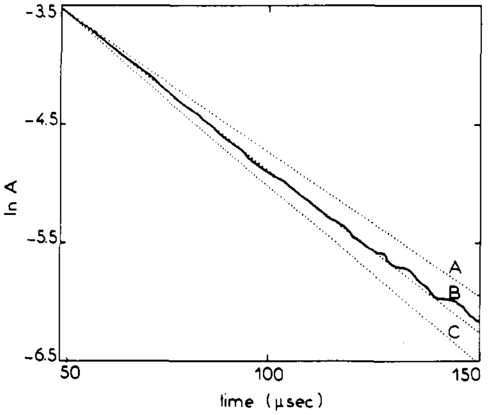

Figure 2. Rate constant k_{O_2} as a function of the number of photolyzing flashes. H_2CO, 40 torr: (◐) 144 and (◑) 29 mtorr of O_2. CH_3CHO, 40 torr: 75 mtorr of O_2, total pressure (O) 45 and (▲) 500 torr. Dotted lines are drawn through points.

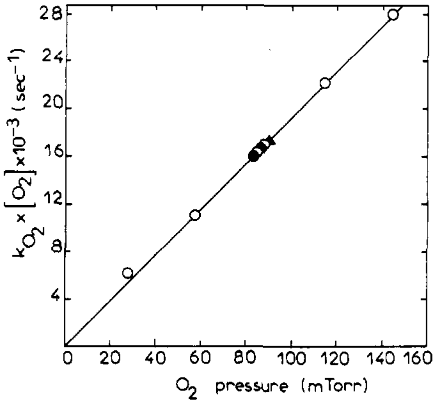

Figure 3. Pseudo-first-order rate constant $k_{O_2} \times [O_2]$ as a function of O_2 concentration: (O) H_2CO, 40 torr; total pressure, 45 torr. (●) CH_3CHO, 40 torr; total pressure, 45 torr. (▲) CH_3CHO, 40 torr; total pressure, 500 torr.

is the path length for the analyzing beam.

The value of the coefficient $2k_3/(\epsilon d)$ was determined in experiments done in the absence of a scavenger: $k_3/\epsilon \approx 6.5 \times 10^7$ cm s^{-1} for H_2CO and $(k_3 + k_6)/\epsilon \approx 19.5 \times 10^7$ cm s^{-1} for CH_3CHO. Therefore, simulated decays of A were fitted to the experimental curves by adjusting only one parameter, the k_x value in eq 9. At the highest pressures of O_2, only minor departures from true pseudo-first-order kinetics are observed (Figure 1). From experiments with no scavenger added, we concluded that HCO does not react with the aldehydes ($k < 10^{-17}$ cm^3 molecule^{-1} s^{-1}).

For each new mixture, the HCO decay was recorded on Polaroid film for successive flashes. Kinetic simulations were then done for each recording, giving a value of k_{O_2}, assuming that the oxygen concentration had not varied from one flash to the next. Typical curves of k_{O_2} vs. the number of flashes clearly show that this assumption is not valid as oxygen consumption is significant (Figure 2). Thus these curves only help in providing a more reliable "first flash" value of k_{O_2} by extrapolating the smoothed curve to the first flash, as we assumed that most of the oxygen is consumed in secondary reactions after the decay (see discussion). The time between flashes was varied from 20 s to 10 min with no noticeable effect on the results of experiments with either scavenger.

Results

Measurements of the rate constant k_{O_2} were performed as a function of oxygen concentration. Figure 3 shows that the plot of $k_{O_2}[O_2]$ vs. $[O_2]$ is linear, as expected in the case of quasi-pseudo-first-order conditions in conjunction with a kinetic simulation. When the total pressure is increased to 500 torr by addition of pure nitrogen, there is no increase of k_{O_2} (see Figure 3, triangle). This is in agreement with the findings of Shibuya et al.[2] and demonstrates that there is no termolecular reaction between HCO and O_2 in this pressure range. The experiments were done with both aldehydes as sources of formyl radicals, with identical results for the k_{O_2} determinations. In our view, this shows that our kinetics simulation scheme adequately describes the HCO decay. The final rate constant $k_{O_2} = (5.6 \pm 0.6) \times 10^{-12}$ cm^3 molecule^{-1} s^{-1} was calculated from the plot in Figure 3. The confidence interval was estimated by analysis of the possible causes of systematic errors. These are mainly of the operational type (pressure measurements, purification of the reagents, and analysis of the kinetic recordings) and account for more than half of the total error in the case of k_{O_2} at room temperature. Mechanistic sources of systematic errors are believed to be negligible as k_x determinations are consistent with both aldehydes for which reaction schemes are known to be different.

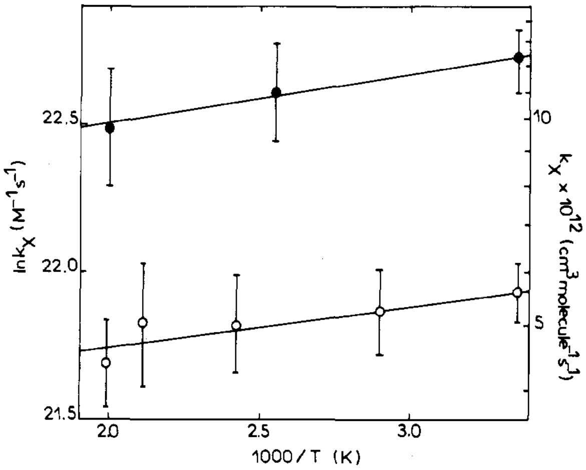

Figure 4. Temperature dependence of k_x: (O) k_{O_2}; (●) k_{NO}. Room-temperature values are averages of many experiments. High-temperature values are single-shot experiments. Error bars express the sums of estimated systematic and random errors.

In O_2 and NO experiments and with both aldehydes, a small residual absorption in the absorption decay was observed. It was interpreted as absorption of some long-lived product (a few ms) that was formed during the decay of HCO. Attempts to assign this absorption to a specific species were not conclusive. In the case of O_2, the absorbing species could be one of those described in the H_2CO photooxidation scheme by Calvert et al.[11] In order to take into account this residual absorption which contributed only one-tenth of the total initial absorption, the base line was raised to the level of the residual absorption.

The effect of the temperature on k_{O_2} is shown in Figure 4 (open circles). There is a slight decrease of k_{O_2} when going to higher temperatures, corresponding to an apparent activation energy of ~−0.3 kcal/mol. This temperature dependence can be better expressed in the form $k_{O_2} = 5.5 \times 10^{-11} \times T^{-0.4\pm0.3}$ cm^3 molecule^{-1} s^{-1}. Random errors for high temperature measurements are estimated from room-temperature kinetics measurements.

The reaction of HCO with NO is known to be faster than that with O_2, and this was confirmed in our experiments from which we determined $k_{NO} = (12.3 \pm 1.2) \times 10^{-12}$ cm^3

---

(11) F. Su, J. G. Calvert, and J. H. Shaw, *J. Phys. Chem.*, **83**, 3185 (1979).

TABLE I

scavenger X	aldehyde	total press., torr	$10^{12}k_X$, cm^3 molecule^{-1} s^{-1}	technique	ref
O_2		4	5.7 ± 1.2	MS[a]	1
	acet[b]	20	6.0 ± 0.9	AS	2
	acet	530	5.3 ± 0.7	AS	2
	form[c]	~10	4.0 ± 0.8	IDLS	3
	acet	13-100	4.0 ± 1.0	IDLS	4
	form	14	3.7 ± 0.8	IDLS	4
	acet	45	5.6 ± 0.9	EAS	*d*
	form	45	5.6 ± 0.6	EAS	*d*
	acet	500	5.6 ± 1.0	EAS	*d*
NO	acet	20	8.6 ± 0.9	AS	2
	acet	530	8.4 ± 0.9	AS	2
	form	~10	14 ± 2	IDLS	3
	form/acet	14-150	12 ± 2	IDLS	4
	form	45	12.3 ± 1.2	EAS	*d*
	acet	45	12.1 ± 1.4	EAS	*d*
	acet	500	12.7 ± 2.0	EAS	*d*

[a] Mass spectrometry. [b] Acetaldehyde. [c] Formaldehyde. [d] This work.

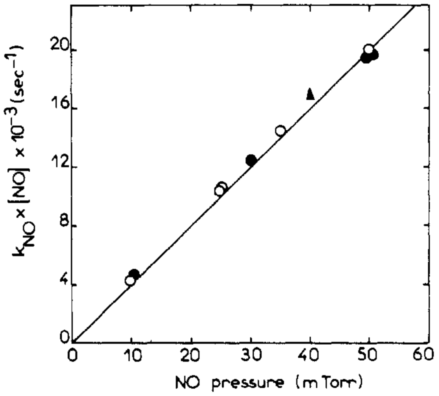

Figure 5. Pseudo-first-order rate constant $k_{NO} \times [NO]$ as a function of NO concentration: (○) H_2CO, 40 torr; total pressure, 45 torr. (●) CH_3CHO, 40 torr; total pressure, 45 torr. (▲) CH_3CHO, 40 torr; total pressure, 500 torr.

molecule^{-1} s^{-1} (Figure 5). We studied carefully the dependence of k_{NO} on the number of photolyzing flashes and found out that NO seemed not to be consumed in the reaction, at least for the first few flashes (Figure 6). This surprising behavior had already been mentioned by Shibuya et al.[2] and will be further discussed below.

As in the case of O_2, no significant effects on k_{NO} were observed upon the variation of the total pressure or the choice of aldehyde (Figure 5). Behavior of k_{NO} as a function of the temperature is similar to that of k_{O_2}, as shown in Figure 4. This temperature dependence can be expressed as $k_{NO} = 1.2 \times 10^{-10} \times T^{-0.4\pm0.3}$ cm^3 molecule^{-1} s^{-1}.

Studies of the reaction of HCO with NO_2 failed because of the total consumption of NO_2 in a single flash. Chain reactions are involved that forbid an accurate rate-constant determination with either aldehyde.

Discussion

In view of the discrepancy in the k_{O_2} and k_{NO} values published to date, this work was aimed at getting more reliable values of k_x and determining its temperature dependence.

Extracavity laser absorption spectroscopy (EAS) was chosen as this technique allows for large pressure and temperature variations. The use of a CW dye laser as the source of the analyzing light improves the sensitivity and the stability of the detection as compared to the use of a flash lamp–spectrograph combination. Moreover, single-shot observation of the HCO decay is an improvement over the point-by-point method used by Shibuya et al.,[2] along with the use of formaldehyde for which kinetic simulations are simpler than those with acetaldehyde.

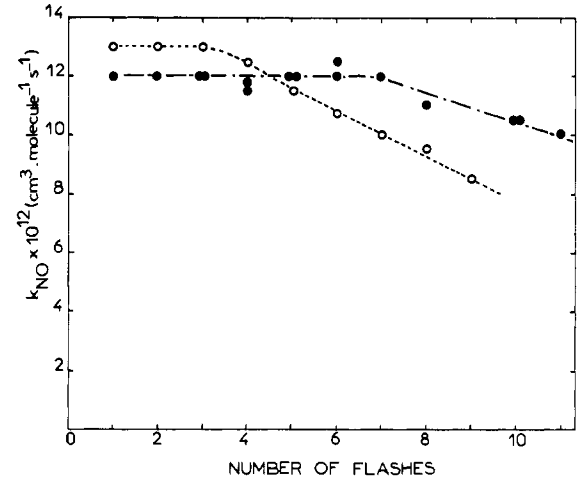

Figure 6. Rate constant k_{NO} as a function of the number of photolyzing flashes. CH_3CHO, 40 torr: (●) 50 mtorr of NO; (○) 30 mtorr of NO. Dotted lines are drawn through points.

The extracavity technique also ensures proportionality between absorbance and concentration. Intracavity methodology, when asssociated with pulsed laser photolysis, cannot yield a homogeneous population of radicals and is very sensitive to diffusion out of the laser beams.[3]

The values of k_{O_2} and k_{NO} available in the literature are listed in Table I. Our k_{O_2} value is in excellent agreement with those obtained by other groups using MS and AS techniques.[1,2] IDLS experiments are in agreement with each other but gave lower values of k_{O_2}. The reason for this disagreement is difficult to assess since similar concentrations of radicals are produced (10^{13}–10^{14} cm^{-3}) and similar O_2 concentration ranges are used (up to 900 mtorr). One possible explanation is that the effect of the successive photolyzing pulses on the oxygen concentration was underestimated in IDLS studies. Oxygen consumption as shown in Figure 1 is greater than that estimated from kinetic simulations. In intracavity experiments this will slow down the decay of HCO as the delay between the photolyzing and analyzing pulses is increased and oxygen concentration is decreasing. On the contrary, our k_{NO} value is in good agreement with these obtained from IDLS measurements, as indicated in Table I. In view of the absence of NO consumption in that case, this agreement is expected. HCO kinetics is not disturbed as successive pulses do not affect appreciably the concentration of NO (Figure 6).

We were unable to explain the absence of NO consumption as reactions of HNO in the gas phase or on the walls should not account for the stability of NO concentration.[9,10] Because of this peculiar phenomenon, the reliability of the k_{NO} value is not as good as for k_{O_2}, although this is not expressed in the estimated error in k_{NO}. There remains an unresolved problem to be tackled.

The observed decrease of k_x with temperature lies within the range of experimental uncertainties but seems to be significant as measurements are reproducible. This behavior is expected for the fast reactions involved and implies that the activation energy is negligible, the temperature dependence being that of the frequency factor.

Apparent negative activation energies have been observed for many radical-radical and radical-molecule reactions. The theory for this phenomenon has not yet been fully developed but should benefit from progress in unimolecular rate theory.

The comparison between near-room-temperature data (~300-500 K) and high-temperature data (~1000-2000 K) is rather difficult because of the lack of reliable high-temperature data and the gap between the two temperature ranges. Flame studies by Peeters et al.[12] yielded a value of k_{O_2} that is 10 times larger than ours, $k_{O_2} = 5 \times 10^{-11}$ cm^3 molecule^{-1} s^{-1} at $1400 < T < 1800$ K, while Westbrook et al.[13] later obtained a lower value for k_{O_2} in their turbulent flow reactor experiment, $k_{O_2} = (2.2 \pm 1.1) \times 10^{-12}$ cm^3 molecule^{-1} s^{-1} at $T = 1100$ K. This latter value fits well on our Arrhenius curve for k_{O_2} determined in the 300-500 K temperature range.

Critical evaluation of the data shown in Table I indicates that k_x values in the higher range are most reliable, and we recommend their use in atmospheric modeling. Despite the lack of accuracy in the k_{O_2} temperature-dependence study, use of our k_{O_2} value in stratospheric modeling is reasonable ($k_{O_2} = (6.2 \pm 0.9) \times 10^{-12}$ cm^3 molecule^{-1} s^{-1} at 228 K). This is to be compared with the lower value recommended in the recent compilation by Hampson[14] (($5.1 \pm 1.3) \times 10^{-12}$ cm^3 molecule^{-1} s^{-1}).

Acknowledgment. We thank Professor J. Joussot-Dubien for his encouraging interest in this work.

---

[12] J. Peeters and G. Mahnen, *Symp. (Int.) Combust., [Proc.]*, **14**, 133 (1973).

[13] C. K. Westbrook, J. Creighton, and C. Lund, *J. Phys. Chem.*, **81**, 2542 (1977).

[14] R. F. Hampson "Chemical Kinetic and Photochemical Data Sheets for Atmospheric Reactions", Vol. 4, 1980, p 47; Report No. FAA-EE-80-17.

ESR Study of Copper Pentanedionate Solutions in Organic Solvents Adsorbed on Porous Silica Gels

Giacomo Martini* and M. Francesca Ottaviani

Institute of Physical Chemistry, University of Florence, 50121 Florence, Italy
(Received: August 27, 1980; In Final Form: February 13, 1981)

The ESR spectra of Cu(acac)$_2$ introduced as a solution in organic solvents (CHCl$_3$, DMF, and pyridine) in different silica gels with pore diameters in the range 4-100 nm are used for the study of the adsorption of both the paramagnetic complex and solvent molecules on the surface where the **g** and the hyperfine splitting constant tensors are modified as a function of interaction with the silica gel substrate. Part of the Cu(acac)$_2$ complex inside the pores maintains liquidlike mobility, while a fraction dependent on the pore size, on the Cu(II) concentration, and on the nature of the solvent gives rise to ESR spectra due to surface-adsorbed species. The ESR parameters and the relative intensity of the liquidlike and surface spectra allow us to suggest that (i) a surface silanol group is coordinated to Cu(acac)$_2$ in the apical position, (ii) the crystal-field strength of the $\equiv$Si—OH group is low compared to that of CHCl$_3$, pyridine, and DMF, and (iii) the DMF molecules are adsorbed on the surface via hydrogen bonds more tightly than the pyridine molecules and CHCl$_3$ is only loosely adsorbed.

Introduction

The preparation and the structure of Cu(II)-containing porous supports have been extensively studied by electron spin resonance (ESR) in the past years with the aim of elucidating the catalytic processes in which such systems are involved.[1-7] Attention was mainly devoted to the localization and bonding features of the surface-adsorbed complexes. However, the study of the mobility of pure fluids or fluid mixtures into fully filled pores of porous supports is also of particular relevance in such fields as heterogeneous catalysis, chromatography, and membrane science. Indeed, the flow rate is in part affected by the interactions of the flowing molecules with the pore walls. These interactions increase with decreasing pore sizes. Calorimetric techniques and adsorption isotherm techniques were extensively used in these researches.[8-10] Also infrared spectroscopy was widely used in spite of the limits imposed by experimental difficulties.[11,12] The ESR of

---

[1] M. Boudart, E. G. Derouane, V. Indovina, and A. B. Walters, *J. Catal.*, **39**, 115 (1975).

[2] Y. Matsunaga, *Bull. Chem. Soc. Jpn.*, **34**, 1291 (1961).

[3] P. A. Berger and J. F. Roth, *J. Phys. Chem.*, **71**, 4307 (1967).

[4] H. Lumbeck and J. Voigtländer, *J. Catal.*, **13**, 117 (1969).

[5] R. G. Herman and R. D. Flentge, *J. Phys. Chem.*, **82**, 720 (1978).

[6] R. Deen, P. I. Th. Scheltus, and G. DeVries, *J. Catal.*, **41**, 218 (1976).

[7] H. Tominaga, Y. Ono, and T. Keii, *J. Catal.*, **40**, 197 (1975).

[8] J. J. Kipling, "Adsorption from Solutions of Electrolytes", Academic Press, New York, 1965.

[9] S. G. Ash, R. Brown, and D. H. Everett, *J. Chem. Thermodyn.*, **5**, 239 (1973).

[10] A. C. Zettlemoyer and K. S. Narayan in "The Solid-Gas Interface", E. A. Flood, Ed., Marcel Dekker, New York, 1967.

[11] L. H. Little, "Infrared Spectra of Adsorbed Species", Academic Press, New York, 1966.

[12] C. H. Rochester, *Adv. Colloid Interface Sci.*, **12**, 43 (1980).

0022-3654/81/2085-1922$01.25/0